

Multi-Dimensional Tunneling in Density-Gradient Theory

M.G. Ancona and K. Lilja¹

Naval Research Laboratory, Washington, DC, ancona@estd.nrl.navy.mil

¹Mixed Technology Associates, LLC, Newark, CA

For engineering-oriented simulations of quantum confinement effects, density-gradient (DG) theory has come into wide use including in multi-dimensions [1]. It is therefore somewhat curious that the DG description of tunneling [2] has not been similarly applied to practical device simulation. The two most important explanations would seem to be (i) questions of principle and (ii) that the existing DG theory is restricted to one-dimensional tunneling for which quantum mechanics (e.g., NEGF) often provides a realistic alternative. In the present work our primary focus is on how tunneling problems can be treated in multi-dimensions in DG theory.

To understand the application of DG theory to elastic tunneling in multi-dimensions it is important to recognize that the relevant equations are better viewed not as a generalization of diffusion-drift theory but as a generalization of ballistic transport theory, i.e., with finite inertia, infinite mobility and zero generation-recombination. The key modification is to include the DG equation of state [2]. To illustrate the approach we consider tunneling across an MIM diode whose electrodes are of arbitrary shape. As described in Ref. 2, the lack of scattering requires that the flow injected from the left electrode be treated separately from the flow injected from the right. Because the electrodes are metals and are isothermal it is reasonable to assume that the tunneling gases are isentropic, isoenergetic and irrotational. Space charge effects are included, however, for simplicity the electrodes are considered to be electrostatically ideal [3]. Under these conditions, the governing equations for the forward-tunneling carriers in steady-state are:

$$\nabla \cdot (n \nabla \vartheta_n) = 0 \quad \nabla \vartheta_n \cdot \nabla \Psi_n^{DG} = 0 \quad \nabla \cdot (b_n \nabla \sqrt{n}) + \frac{\sqrt{n}}{2} (\psi + \Psi_n^{DG}) = 0 \quad \nabla^2 \psi = \frac{q}{\epsilon_d} (n + u)$$

where n and u are the forward and backward tunneling electron density, respectively, ϑ_n is the velocity potential and Ψ_n^{DG} is the total enthalpy. With appropriate boundary condition appended, these equations and similar ones for the backward-tunneling gas can be solved and the tunneling current determined. As an example, in Fig. 1 we model a 1-D MIM structure and find good agreement between DG simulation and a well-known approximate formula of Simmons [4].

To solve the DG tunneling equations in multi-dimensions numerical methods are required. To this end, we have implemented the equations in the code PROPHET from Mixed Technology Associates, LLC. We consider ridge and STM-like tip electrode geometries with ultra-small curvature and separated by a dielectric from planar electrodes (Fig. 2). The ridges (2D) and tips (3D) are assumed Lorentzian in shape as defined in Fig. 2. Figures 3-5 show simulation results for the 2D ridge geometry with $d = 1.5\text{nm}$ and a chemical potential barrier height of 2eV. Note the existence of an asymmetry in the I-V characteristics (Fig. 3) that originates in the geometrical asymmetry as discussed by Lucas [5]. In Fig. 6 we compare I-Vs for a 2-D ridge and a 3-D tip each having the same parameters; a stronger geometrical asymmetry is evident in the 3D case.

Acknowledgement: MGA thanks ONR for funding support.

1. For example, the DG treatment of carrier confinement is implemented in the commercial simulators available from Synopsys, Silvaco and ISE.

2. M.G. Ancona, *Phys. Rev. B* **42**, 1222 (1990).
3. M.G. Ancona, *Phys. Rev. B* **46**, 4874 (1992).
4. J.G. Simmons, *J. Appl. Phys.* **34**, 1793 (1963).
5. A.A. Lucas *et al*, *Surf. Sci.* **269/270**, 74 (1992).

A full journal publication of this work will be published in the Journal of Computational Electronics.

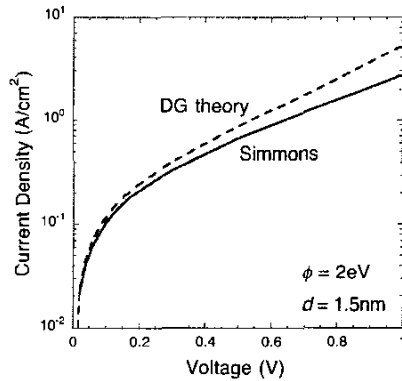


Fig. 1. Comparison of DG simulation and formula of Simmons [4] for 1D MIM tunneling with space charge neglected.

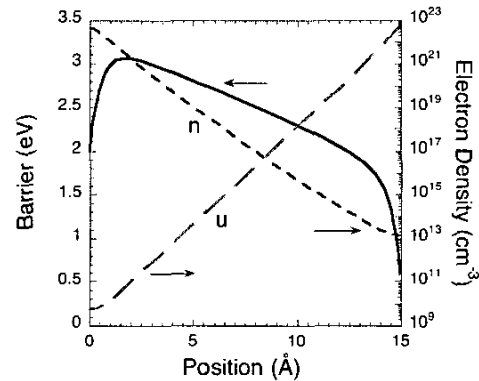


Fig. 4. DG profiles of the electron densities and barrier along the centerline with $a = 1\text{nm}$.

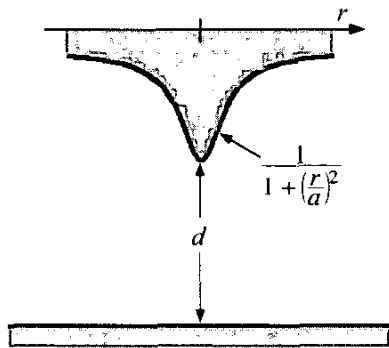


Fig. 2. Schematic of an MIM diode with a ridge or tip electrode geometry.

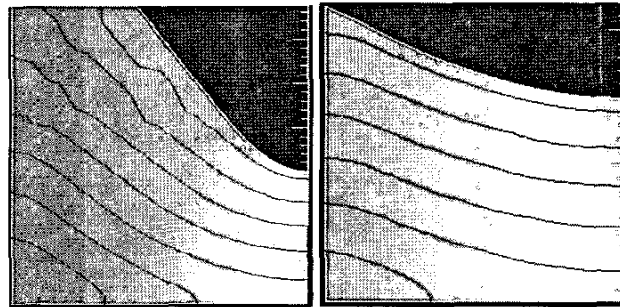


Fig. 5. Ridge geometry, concentration (contour lines: 10^{10} - 10^{22}cm^{-3}), and current density (color coded) for electrons tunneling from the 2D ridge to the plane with $V = -1.5\text{V}$ and (left) $a = 1.5\text{nm}$, and (right) $a = 5\text{nm}$.

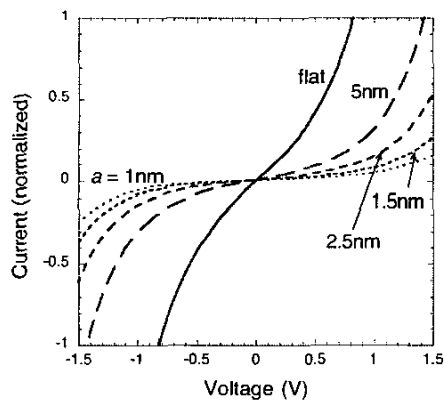


Fig. 3. 2D simulation of the tunneling current for ridge electrodes of varying widths (a) and normalized to the planar case.

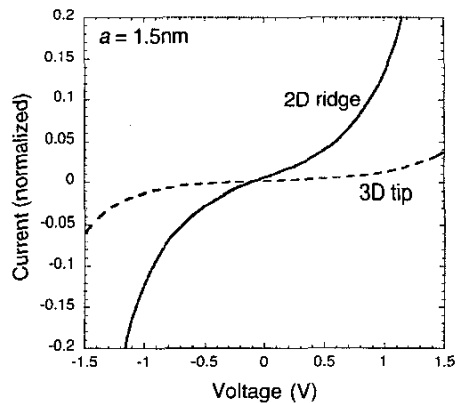


Fig. 6. Comparison of simulated tunneling currents from a 3D tip electrode with a 2D ridge electrode.

A full journal publication of this work will be published in the Journal of Computational Electronics.